# Generating single attosecond pulse using multi-cycle lasers in a polarization gate

**Valer Tosa[1],* Katalin Kovacs[1], Carlo Altucci[2], and Raffaele Velotta[2]**

[1]*National Institute for Research and Development of Isotopic and Molecular Technologies, Donath str. 65-103, 400293 Cluj-Napoca, Romania*
[2]*Dipartimento Scienze Fisiche, Universita "Federico II", Complesso Monte Santangelo, via Cinthis, 80126 Napoli, Italia*
**tosa@itim-cj.ro*

**Abstract:** We analyze the macroscopic effects which are responsible for producing clean isolated pulses lasting few hundreds of attoseconds when starting from multi-cycle fundamental pulses. In particular, we consider a polarization gating scheme and show that, at high fundamental peak intensities, in the range 0.7-1 PWcm$^{-2}$, it usually produces three-four main attosecond pulses of radiation at single dipole level, just located in the leading edge of the laser pulse. We describe the physical mechanisms contributing to the formation of a single attosecond pulse by using a three dimensional non-adiabatic model and a quantum trajectory phase calculation. An analysis of the scheme optimization and stability against various parameters is performed in view of an experimental scheme implementation.



**OCIS codes:** OCIS codes: (020.2649) Strong field laser physics; (190.4160) Multiharmonic generation; (320.2250) Femtosecond phenomena; (320.7110) Ultrafast nonlinear optics

## References and links

1. P. M. Paul, E. S. Toma, P. Breger, G. Mullot, F. Auge, Ph. Balcou, H. G. Muller, and P. Agostini, "Observation of a train of attosecond pulses from high harmonic generation," Science **292**(5522), 1689–1692 (2001).
2. M. Hentschel, R. Kienberger, Ch. Spielmann, G. A. Reider, N. Milosevic, T. Brabec, P. Corkum, U. Heinzmann, M. Drescher, and F. Krausz, "Attosecond metrology," Nature **414**(6863), 509–513 (2001).
3. P. B. Corkum, and F. Krausz, "Attosecond science," Nat. Phys. **3**(6), 381–387 (2007).
4. P. H. Bucksbaum, "The future of attosecond spectroscopy," Science **317**(5839), 766–769 (2007).
5. P. Baum, and A. H. Zewail, "Attosecond electron pulses for 4D diffraction and microscopy," Proc. Natl. Acad. Sci. U.S.A. **104**(47), 18409–18414 (2007).
6. A. L. Cavalieri, N. Müller, T. Uphues, V. S. Yakovlev, A. Baltuska, B. Horvath, B. Schmidt, L. Blümel, R. Holzwarth, S. Hendel, M. Drescher, U. Kleineberg, P. M. Echenique, R. Kienberger, F. Krausz, and U. Heinzmann, "Attosecond spectroscopy in condensed matter," Nature **449**(7165), 1029–1032 (2007).
7. P. B. Corkum, "Plasma perspective on strong field multiphoton ionization," Phys. Rev. Lett. **71**(13), 1994–1997 (1993).
8. R. Kienberger, E. Goulielmakis, M. Uiberacker, A. Baltuska, V. Yakovlev, F. Bammer, A. Scrinzi, T. Westerwalbesloh, U. Kleineberg, U. Heinzmann, M. Drescher, and F. Krausz, "Atomic transient recorder," Nature **427**(6977), 817–821 (2004).
9. I. P. Christov, M. M. Murnane, and H. C. Kapteyn, "High-harmonic generation of attosecond pulses in the "single-cycle" regime," Phys. Rev. Lett. **78**(7), 1251–1254 (1997).
10. C. A. Haworth, L. E. Chipperfield, J. S. Robinson, P. L. Knight, J. P. Marangos, and J. W. G. Tisch, "Half-cycle cutoffs in harmonic spectra and robust cerrier-envelope phase retrieval," Nat. Phys. **3**(1), 52–57 (2006).
11. C. Altucci, C. Delfin, L. Roos, M. B. Gaarde, A. L'Huillier, I. Mercer, T. Starczewski, and C.-G. Wahlström, "Frequency-resolved time-gated high-order harmonics," Phys. Rev. A **58**(5), 3934–3941 (1998).
12. O. Tcherbakoff, E. Mével, D. Descamps, J. Plumridge, and E. Constant, "Time-gated high-order harmonic generation," Phys. Rev. A **68**(4), 043804 (2003).
13. G. Sansone, E. Benedetti, F. Calegari, C. Vozzi, L. Avaldi, R. Flammini, L. Poletto, P. Villoresi, C. Altucci, R. Velotta, S. Stagira, S. De Silvestri, and M. Nisoli, "Isolated single-cycle attosecond pulses," Science **314**(5798), 443–446 (2006).
14. L. J. Sola, E. Mével, L. Elouga, E. Constant, V. Strelkov, L. Poletto, P. Villoresi, E. Benedetti, J. P. Caumes, S. Stagira, C. Vozzi, G. Sansone, and M. Nisoli, "Controlling attosecond electron dynamics by phase-stabilized polarization gating," Nat. Phys. **2**(5), 319–322 (2006).
15. S. Gilbertson, H. Mashiko, C. Q. Li, E. Moon, and Z. H. Chang, "Effects of laser pulse duration on extreme ultraviolet spectra from double optical gating," Appl. Phys. Lett. **93**(11), 111105 (2008).

#112585 - $15.00 USD Received 9 Jun 2009; revised 24 Jul 2009; accepted 27 Jul 2009; published 18 Sep 2009

16. M. Nisoli, S. De Silvestri, O. Svelto, R. Szipöcs, K. Ferencz, Ch. Spielmann, S. Sartania, and F. Krausz, "Compression of high-energy laser pulses below 5 fs," Opt. Lett. **22**(8), 522–524 (1997).
17. P. Tzallas, E. Skantzakis, C. Kalpouzos, E. P. Benis, G. D. Tsakiris, and D. Charalambidis, "Generation of intense continuum extreme-ultraviolet radiation by many-cycle laser fields," Nat. Phys. **3**(12), 846–850 (2007).
18. C. Altucci, R. Esposito, V. Tosa, and R. Velotta, "Single isolated attosecond pulse from multicycle lasers," Opt. Lett. **33**(24), 2943–2945 (2008).
19. H. J. Shin, D. G. Lee, Y. H. Cha, K. H. Hong, and C. H. Nam, "Generation of nonadiabatic blueshift of high harmonics in an intense femtosecond laser field," Phys. Rev. Lett. **83**(13), 2544–2547 (1999).
20. D. Oron, Y. Silberberg, N. Dudovich, and D. M. Villeneuve, "Efficient polarization gating of high-order harmonic generation by polarization-shaped ultrashort pulses," Phys. Rev. A **72**, 063816(R) (2006).
21. C. Altucci, V. Tosa, and R. Velotta, "Beyond the single-atom response in isolated attosecond-pulse generation," Phys. Rev. A **75**, 061401(R) (2007).
22. V. Tosa, K. T. Kim, and C. H. Nam, "Macroscopic generation of attosecond-pulse trains in strongly ionized media," Phys. Rev. A **79**(4), 043828 (2009).
23. G. Sansone, "Quantum path analysis of isolated attosecond pulse generation by polarization gating," Phys. Rev. A **79**(5), 053410 (2009).
24. V. Tosa, H. T. Kim, I. J. Kim, and C. H. Nam, "High-order harmonic generation by chirped and self-guided femtosecond laser pulses," Phys. Rev. A **71**(6), 063807 (2005).
25. M. Lewenstein, Ph. Balcou, M. Yu. Ivanov, A. L'Huillier, and P. B. Corkum, "Theory of high-harmonic generation by low-frequency laser fields," Phys. Rev. A **49**(3), 2117–2132 (1994).
26. M. V. Ammosov, N. B. Delone, and V. P. Krainov, "Tunnel ionization of complex atoms and of atomic ions in an alternating electromagnetic field," Sov. Phys. JETP **64**, 1191–1194 (1986).
27. D. B. Milosevic, G. G. Paulus, and W. Becker, "Ionization by few-cycle pulses: Tracing the electron orbits," Phys. Rev. A **71**(6), 061404 (2005) (and references therein).
28. M. B. Gaarde, and K. J. Schafer, "Generating single attosecond pulses via spatial filtering," Opt. Lett. **31**(21), 3188–3190 (2006).
29. P. Salières, A. L'Huillier, and M. Lewenstein, "Coherence control of high-order harmonics," Phys. Rev. Lett. **74**(19), 3776–3779 (1995).
30. Z. Chang, A. Rundquist, H. Wang, I. Christov, H. C. Kapteyn, and M. M. Murnane, "Temporal phase control of soft-x-ray harmonic emission," Phys. Rev. A **58**(1), R30–R33 (1998).
31. M. B. Gaarde, F. Salin, E. Constant, Ph. Balcou, K. J. Schafer, K. C. Kulander, and A. L'Huillier, "Spatiotemporal separation of high harmonic radiation into two quantum path components," Phys. Rev. A **59**(2), 1367–1373 (1999).

## 1. Introduction

The first generation of an attosecond pulse train [1] followed by the measurement of a single isolated attosecond pulse (SAP) [2] has paved the way to what has been called attoscience [3], whose aim is the investigation of physical phenomena occurring on a time scale comparable to the electron revolution time around the nucleus in the Bohr's vision of the atom. Since the electrons trigger or mediate virtually all processes in atoms, molecules and condensed matter, formidable outcomes are expected in chemistry [4], biology [5] and materials science [6]. So far sub-femtosecond pulses have been mainly generated by means of High Harmonic Generation (HHG) in gases, which can be described by the three-step model [7]. In the first step the electron tunnels through the Coulomb-like potential barrier lowered by the laser electric field, then gains kinetic energy moving in the laser ponderomotive potential, and finally returns to the vicinity of the ionic core where it recombines and emits an extreme ultraviolet (XUV) photon. It turns out that SAP can only be obtained if one is able to select the HHG emission within half a cycle of the laser field. With few cycle laser pulses this was achieved either by selecting spectrally [2,8,9] or spatially [10] the harmonics generated in a half cycle by linearly polarized pulses or by using the polarization gating technique [11,12], which exploits the fact that a nonlinear polarization of the pumping field prevents the electron from re-colliding [13,14].

A huge breakthrough for obtaining SAPs would be represented by the use of multi-cycle, rather than few-cycle laser sources, due to their much higher energy per pulse and commercial availability. Lately, based on a two-colour double-optical gating scheme, attempts were made to generate SAPs by means of 8-12 fs driving Titanium: Sapphire pulses [15]. Nevertheless, though slightly longer than few-cycle, such high-energy IR-pulses cannot be considered the solution to the problem yet, since they are not commercially available, rather they are obtained through the non-trivial hollow fibre compression technique [16]. Recently, a polarization gating technique based on an interferometric modulation of the ellipticity of a 50-

#112585 - $15.00 USD Received 9 Jun 2009; revised 24 Jul 2009; accepted 27 Jul 2009; published 18 Sep 2009

fs-long driving pulse has been put forward [17] leading to a continuum XUV spectrum, which might be possibly associated to a SAP. The method generates the linear polarization gate only in the central part of the driving pulse which imposes severe limitations both on the duration and the energy of the driving pulse since medium ionization has to be kept as low as possible before HHG occurs. Indeed, for high ionization levels, the plasma would significantly alter the driving pulse in the gate which, together with a strong depletion of the gas target, would impede an efficient HHG, thereby hampering an efficient generation of the SAP.

Recently we proposed a new approach [18] to achieve SAP from multi-cycle pulses delivered by commercial laser systems (Titanium: Sapphire sources with central wavelength at 800 nm), which combines a polarization gating generated in this case on the leading edge of the driving pulse with a subsequent ionization gating [19] whose role is to prevent the emission of additional attosecond pulses from the rest of the pulse. Such a method shows to be effective with pulse durations up to 25 fs and can be used with actual intensities as high as 1 PW·cm$^{-2}$ or potentially more, thereby overcoming a technical limitation arising when Spatial Light Modulator [20] is used to generate a polarization gate.

Here we focus on studying in detail the physical mechanisms underlying SAP generation reported in [18] and present a systematic analysis of the role played by the main physical parameters in the above phenomenon in order to maximize the spectral brightness of the generated SAP. A key role in the effectiveness of our method is played by both the fundamental and the harmonic field propagation which acts as a spatial filtering and contributes to the generation of a clean SAP [21, 22].

We mention that the polarization gating scheme proposed in [14] was recently analyzed [23] using the stationary phase approximation to generate and explore quantum trajectories of electrons. The approach is similar to the present one, but it does not allow for trajectory calculations in an arbitrary-shape driving pulse. In consequence it is also not suitable to include propagation effects which would be very important if we want to find the optimal phase-matching conditions.

The paper is constituted by three sections after this introduction. The first section is dedicated to review and further enlighten the scheme proposed in [18], followed in the second section by a reminder of the modeling tools utilized to carry on our analysis. The third section has a first part in which the formation mechanism of the SAP and single electron trajectories contributing to the SAP are discussed, followed by a second part in which we analyze the technical limits of the method and estimate the final SAP brightness.

## 2. Polarization gate

The key idea to produce XUV SAP with multi-cycle optical pulses is to induce a single half optical cycle time window of nearly linear polarization in the leading edge of the driving pulse. This window must happen at the maximum possible laser intensity for HHG to take place before the significant medium ionization occurs.

In principle our method assumes that two copies of a linearly polarised, multi-cycle laser pulse are delayed and differently chirped, then superimposed with crossed polarisation in a single Michelson interferometer (see [18] for details). A frequency modulation (chirping) of one beam is possibly achieved by self-phase modulation (SPM) which occurs when the beam crosses a piece of suitable material. We stress that frequency modulation by SPM is to be preferred to that introduced through dispersion because it can easily provide a large amount of chirp while keeping constant the pulse duration. Actually, the dispersion should be kept as low as possible in order to preserve the pulse duration. Eventually, the output of the interferometer is the superposition of the two beams. If one starts from a Gaussian-type beam, the chirped and delayed beam can be described by the following equation:

$$E_y\left(t,r,z\right)=E_{0y}\exp\left[-1.39\left(\frac{t-T_d}{\tau_p}\right)^2\right]\sin\left[-\omega_0\left(t-T_d\right)+\frac{2\pi\mathrm{L}}{\lambda}n_2I\left(t-T_d\right)-\zeta\left(r,z\right)+\varphi_{0y}\right].\quad(1)$$

#112585 - $15.00 USD Received 9 Jun 2009; revised 24 Jul 2009; accepted 27 Jul 2009; published 18 Sep 2009

In Eq. (1) $E_{0y} = E_0 / \sqrt{2}$, $E_0$ is the input electric field amplitude, $T_d$ is the relative delay between the output pulses, $\tau_p$ is the input pulse duration (Full Width at Half Maximum), $\omega_0$ is the central oscillation frequency, $\zeta(r,z)$ is the spatial phase and $\varphi_{0y}$ is the carrier to envelope phase (CEP). Likewise $E_x(r,z,t)$ is described by Eq. (1) without SPM term, with $E_{0x} = E_0 / \sqrt{2}$ and setting $T_d = 0$. The variation of the ellipticity (see next section) reveals that this configuration generates more gates of linear polarization in which harmonic generation could potentially occur. However, earlier gates are not suited for HHG because they experience too small field intensity, whereas later gates, in the trailing edge of the laser pulse, do not contribute to HHG because they experience a fully depleted medium due to very high tunnel ionization.

A robust SPM provides the required chirp and broadens the initial spectrum centred at 800 nm towards the infrared (leading edge) and the visible (trailing edge). In view of the role played by the ionization gating only the first half of the pulse needs to be preserved in terms of spectral and temporal quality. To this end, the main effect to be considered is the group velocity dispersion (GVD) occurring in all the crossed optics, which would lead to pulse lengthening. Since in our method the single attosecond pulse is generated in the leading edge of the chirped pulse, we can neglect GVD contribution because its importance tends to vanish for wavelengths longer than 800 nm in most materials. However, possible residual positive GVD can be corrected through negative dispersive systems (e.g. pairs of prisms or diffraction gratings).

## 3. Modeling tools

We analyzed the above polarization gate configuration by using a three dimensional non-adiabatic model. The modeling [24] includes three necessary steps: (i) solving the propagation equation for the laser field in an ionized medium, (ii) calculating the single dipole developed in the interaction between the atom and the propagated field, and finally (iii) calculating the harmonic field generated by the single dipoles in the interaction region. This model allows us to estimate the macroscopic response of the gaseous medium in conditions very close to the experimental ones.

In ionized gases the laser pulse propagation is described by the wave equation which can be written as:

$$\nabla^2 \vec{E}(r,z,t) - \frac{1}{c^2}\frac{\partial^2 \vec{E}(r,z,t)}{\partial t^2} = \frac{\omega^2}{c^2}(1-\eta_{eff}^2)\vec{E}(r,z,t), \quad (2)$$

where $\vec{E} = E_x\vec{i} + E_y\vec{j}$ is the transverse electric field propagating in $z$ direction, both components on $x$- and $y$-axis having central frequency $\omega_0$. The effective refractive index of the medium $\eta_{eff}(r,z,t)$ accounts for refraction, absorption, optical Kerr effect, as well as for the presence of electron plasma. We solve a similar propagation equation for the harmonic field in which the free term contains the dipole of the single atom. This term is calculated by using the strong field approximation (SFA) [25]. More details on calculations can be found elsewhere [24]. We only mention here that Eq. (2) was solved separately for the two components $E_x$ and $E_y$ because they propagate independently but in a common refractive index mainly determined by the electron plasma created by the total field $\vec{E}$ and calculated using a non-adiabatic version of the Ammosov-Delone-Krainov approximation [26].

Most information and phenomenological insight regarding the mechanisms leading to HHG can be obtained by examining the trajectories of electrons contributing to a $q^{\text{th}}$ order harmonic photon emission. The most probable trajectory of an electron that ionizes at time $t$, travels in the laser field, then recombines at time $t'$ occurs under the condition of stationary phase. The constraints for having stationary phase leads to the following saddle-point equations (see [25] for a detailed saddle-point analysis):

#112585 - $15.00 USD Received 9 Jun 2009; revised 24 Jul 2009; accepted 27 Jul 2009; published 18 Sep 2009

$$
\begin{aligned}
&\frac{\vec{\alpha}(t)-\vec{\alpha}(t')}{t'-t} = \vec{p} \\
&\left[\vec{p}+\vec{A}(t)\right]^2 = 2\mathrm{I}_p \qquad , \\
&\left[\vec{p}+\vec{A}(t')\right]^2 = 2(q\omega - I_p\,)
\end{aligned} \tag{3}
$$

where $\vec{A}$ is the vector potential of the field with $\vec{E} = -d\vec{A}\,/\,dt$, and $\vec{\alpha}(t) = \int A(t')dt'$, while $\vec{p}$ is the canonical momentum. The first saddle-point equation in Eq. (3) expresses the return condition for the electron while the second and third equations express the energy conservation at the ionization and recombination time, respectively.

Previous papers [27] were published on this topic, but in all cases the authors make use of analytical calculations assuming that the radiation propagates as a plain wave and its electric field component has an expression that can be handled analytically. In experiments and practical applications, however, laser pulses are usually tailored to a complex spatial-temporal shape and spatial-spectral profile in order to meet specific requirements. Moreover, the initial pulse can suffer distortions due to its propagation in an ionized medium. Analytical calculations completely fail when one wants to trace electron trajectories developed in such realistic fields. To overcome this inconvenience we developed a numerical method which allows calculation of the so-called "quantum trajectories" for an arbitrary electric field, provided it is given numerically as a function of time. We solve the above nonlinear system of equations for the canonical momentum and for the birth and recollision times $t$ and $t'$. Since $I_p < 0$ it results immediately that all the solutions will be complex. Rearranging the equations and separating the real and imaginary parts, the system of equations becomes a set of four equations which was solved numerically to yield the real and imaginary part of the birth and recollision time. The phase for a trajectory generating harmonic of order $q$ was calculated as:

$$
\phi_k^{(q)} = q\omega_0 t_k^{'} - \int_{t_k}^{t_k^{'}} \left( \frac{[\vec{A}(t'') - \vec{A}(t)]^2}{2} + I_p \right) dt'', \tag{4}
$$

where $k$ identifies a specific burst in time, while $I_p$ is the ionization potential of the parent atom. Using Eq. (4) one can calculate the phase for a class of short or long trajectories in a specific optical cycle. All trajectories fulfilling these conditions will contribute to the same attosecond burst thus their phases can be used to estimate the phase-matching (PM) condition for that burst. One can go further and calculate the coherence length $L_c$ corresponding to a variation $\delta\varphi$ of the phase $L_c = \pi/\ \delta k = \pi z\ /\ \delta\varphi$. In this paper we will show that the PM analysis should be performed for every burst generated at single dipole level as it experiences different PM conditions along the propagation direction. A similar analysis was used to describe PM in generating attosecond pulse trains [22], but here the trajectories are generated using the saddle point equations rather than classical.

### 4. Results and discussion

The initial stage of investigation was devoted to finding the range of the key parameters (chirp, CEP, and delay) which determine the formation of the SAP. In order to have the gate of linear polarization in correlation with the ionization dynamics, the choice of peak intensity and pulse duration is also important. The result presented here concerns the optimized case of two pulses having an energy of 0.23 mJ and a duration of 20 fs each, with a relative delay of 0.32 fs, irradiating an up to 4 mm-long Ar jet in a 60 cm focal length geometry. In such conditions the peak intensity at focus amounts to about 0.48 $\mathrm{PWcm}^{-2}$ in each pulse. The jet having $3.3\times10^3$ Pa local pressure is placed 1.7 mm after the focus. At the entrance of the interaction region an initial Gaussian shape is assumed for both spatial and temporal profile of the two pulses.

#112585 - \$15.00 USD Received 9 Jun 2009; revised 24 Jul 2009; accepted 27 Jul 2009; published 18 Sep 2009

The maximum SPM-induced phase shift experienced by the $E_y$ electric field has been assumed to be 9 rad. It is worth to notice that the value of 9 rad for the SPM-induced phase variation is a trade-off between a higher value which would generate more cusp points, and a lower value which would broaden the single time window at a cusp point. In both cases multiple attosecond pulses would be produced. It is also worth stressing that in a first stage we neglected a possible spatial variation of the induced SPM, due to radial modulation of the pulse intensity. Such an assumption relies on the possibility to shape a top-hat spatial mode for the input beam, what could be easily obtained by enlarging the beam size and then selecting only its central part, for instance.

*4.1 Mechanism of SAP formation*

We first present the results obtained in modeling the formation of SAP, as these results allow us to understand the physical mechanism behind this formation and to validate, at least at theoretical level, the method proposed for obtaining SAP from multi-cycle lasers.

Given in Fig. 1(a). (thick black curve) is the total (radially integrated) near field emitted after 1-mm of propagation though the gas target. It shows a single emission at about three optical cycles before pulse center, and an additional spurious peak in the tail of the pulse. The time dependent ellipticity (dashed line in Fig. 1(a).) of the laser field shows that these two peaks correspond to the two gates of linear polarization. However, if we analyze the single dipole developed on-axis along the propagation coordinate, we see in Fig. 1(b). that the emitted radiation consists of three main bursts, labeled B1, B2, and B3 in the plot, which are developed in the time interval ($-4T_0$, $-2T_0$), with $T_0=2\pi/\omega_0$. For z=0, i.e. at the gas medium entrance, the emission is confined in this time interval because of the combined effect of polarization gate and ionization. Indeed, for the intensity produced at z=0 the depletion is complete towards the pulse center, as shown by the red curve in Fig. 1(a). For z>0 the dipole response changes and these modifications are roughly proportional to the distance traveled in the medium, which is a first indication of the presence of an essential propagation effect. Moreover, it also depends on the moment of emission: the first burst emitted at $t=-3.1T_0$ best preserves its emission time along z, while later peaks B2 and B3 shift their emission in time while propagation carries on. For a given z, the later the emission the larger the shift is.

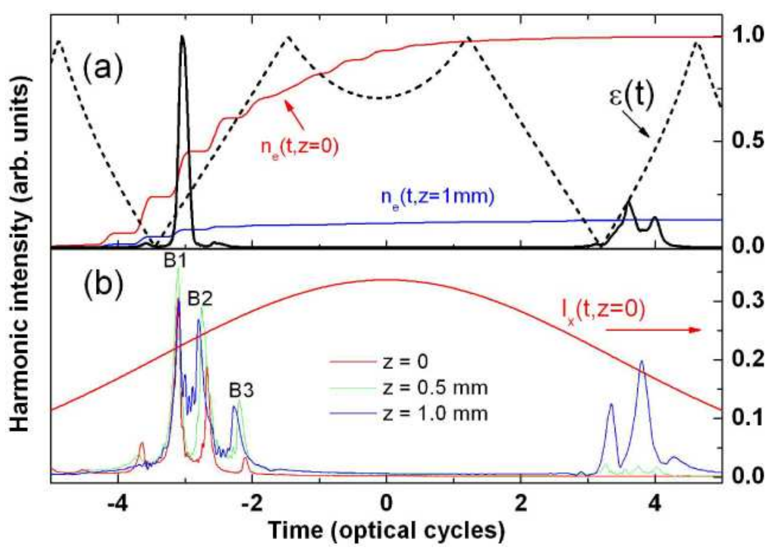


Fig. 1. (a) Final near field generated by the proposed scheme (black thick line) The on-axis electron fraction at the entrance (red solid line) and exit (blue solid line) of the interaction region, as well as the field ellipticity ε(t) (dot line) are also plotted. (b) Time dependence of the single dipole emitted on-axis at different distances of propagation, as specified in the legend. Three main bursts, labeled B1, B2, and B3 are emitted but only B1 survives after propagation. The field intensity (in $PWcm^{-2}$) on x-axis is also shown by the red thick line.

#112585 - $15.00 USD Received 9 Jun 2009; revised 24 Jul 2009; accepted 27 Jul 2009; published 18 Sep 2009

For propagation distances z>0.5 mm an additional emission appears in the interval ($3T_0$, $4T_0$), corresponding to the next gate of linear polarization located in the trailing edge of the pulse. This emission occurs because, due to the defocusing, the laser intensity decreases from 0.35 to 0.2 $PWcm^{-2}$, which induces in turn a decrease of the plasma density by a factor of ten, as seen by the blue line in Fig. 1(a). The pulse is formed in the tail of the laser pulse which is strongly defocused by the electron plasma during propagation. As a result the harmonic field generated will also be emitted under a larger divergence, and, as it will be shown later, can be eliminated by placing an iris of appropriate aperture in the far field.

The quantum trajectory calculation, performed within the saddle-point approximation, reveals the detailed mechanism of the SAP formation. We analyzed the trajectories generated by the combined action of the two fields and studied the influence of the fields' propagation on their phases and their conditions of generation. This helps us to understand the burst selection during propagation and the dependence of this process on the birth moment. In Fig. 2. there are plotted the phases of the trajectories generating the 23rd order harmonic (H23), and their dependence on the propagation distance. Both trajectories contributing, originating from B1 and B2 bursts, are plotted. One can immediately see that only the phases of the short trajectories in the B1 burst fulfill the condition for PM propagation of H23. The coherence length, i.e. the distance over which the phase changes by π radians, is initially 0.4 mm but in the z range from 0.5 to 2 mm is larger than 2 mm which means a PM regime for B1. This result is consistent with the result obtained from the full calculation of the harmonic field which indicates that the maximum yield for B1 burst is obtained for a medium length of 2 mm. In addition, quantum trajectory analysis clarifies the origin of different bursts. Burst B1 is built from short trajectories which survive along the whole propagation distance and this explains its high intensity. Burst B2 develops only in a limited range of the fundamental pulse propagation from the short trajectories which have larger phase variation and this is the reason why it results weaker in intensity.

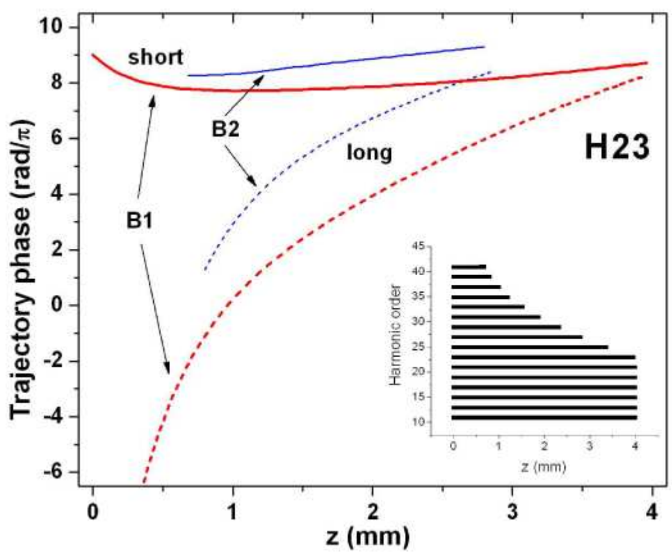


Fig. 2. Phases of the trajectories generating H23 on-axis along the propagation direction. Short and long trajectories contributing to the most intense bursts in Fig. 1(b)., emitted at $t=-3.1T_0$ (B1) and $t=-2.6T_0$ (B2) are included. The inset shows the extension of the trajectories generating the harmonics from H11 to H41.

Here we would like to emphasize that this kind of time-dependent PM analysis based on the calculation of quantum trajectories is performed for the first time, thanks to the possibility to obtain quantum trajectories generated by laser pulse having an arbitrary temporal shape. This instrument is especially useful when analyzing polarization gate configurations in which

#112585 - $15.00 USD Received 9 Jun 2009; revised 24 Jul 2009; accepted 27 Jul 2009; published 18 Sep 2009

the HHG takes place in a very limited time window, so the trajectory itself and its phase is very sensitive to the parameters of the two fields.

For the B1 burst a similar phase variation was obtained for all trajectories generating harmonics in the range H13-H41. This indicates a good build-up of these harmonics, therefore an intense resulting burst. For the B2 burst both the long and the short trajectories will have larger phase variations for all contributing harmonics. The best (short trajectory) coherence length for this burst is shorter than 1 mm so this burst will not experience favorable conditions for building-up. It is interesting to note, as shown in the inset of Fig. 2. for B1 burst, that the spectral structure of the bursts changes along *z* For longer propagation distances higher order harmonics gradually disappear, due to the decrease of the generating intensity. If for z=0 harmonics from H11 to H41 contribute, for z=4 mm the range is from H11 to H23. The situation is worse for burst B2: from H29 to H35 for z=0, but only from H11 to H15 for z=4 mm. In fact, from Fig. 2. one can see that H23 only exists in a limited z range, from 0.6 to 2.6 mm.

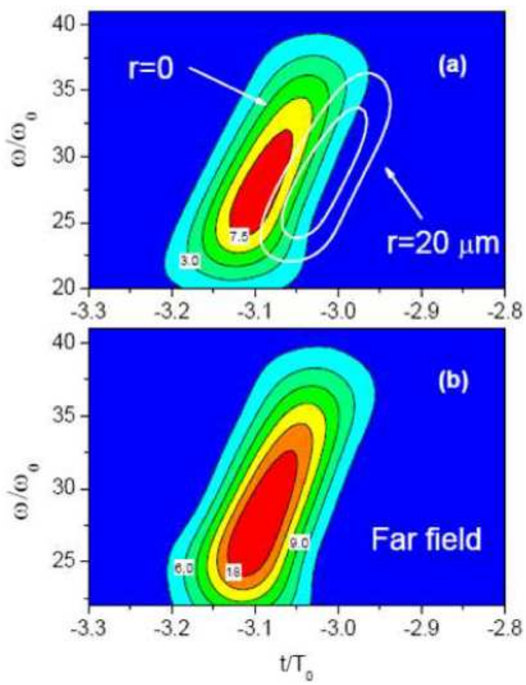


Fig. 3. Spectrogram of the harmonic field producing the B1 burst: (a) near field for the on-axis and 20 µm off-axis emission, (b) on-axis far field.

The change in the spectral components contributing to the SAP formation along with the propagation coordinate might influence the time-frequency structure of the final attosecond pulse and impart some degree of chirp. To estimate the spectral structure of the generated burst we performed a time-frequency analysis of the harmonic field, by calculating the short time Fourier transform [24]: if $H(t)$ is the time signal under inspection, we apply a window function $g(t)$ which is sliding along the signal $H(t)$ and for each shift $g(t–t')$ we compute the usual Fourier transform of the product function $H(t')g(t–t')$. The square of the resulting time-frequency distribution is called a spectrogram and was calculated for the harmonic field contributing to B1 burst, for the near field both on-axis and 20 µm off-axis (Fig. 3(a).) as well as for the far field (Fig. 3(b).) on-axis. One can estimate that for the near field the positive chirp is about 120 $fs^{-2}$ for the on-axis and slightly larger for the field at 20 µm. The temporal delay between the two distributions is about 160 as which is important when estimating the chirp of the emitted overall field as well as its duration. In particular, this indicates that radial

#112585 - $15.00 USD Received 9 Jun 2009; revised 24 Jul 2009; accepted 27 Jul 2009; published 18 Sep 2009

modulations of the laser intensity also imply a non-negligible SAP lengthening. In order to reduce such a lengthening and to obtain the shortest possible SAP duration one should use a top-hat spatial mode. This delay corresponds to a dependence of the recollision time on the radial coordinate, through the laser field intensity distribution. Indeed, as the laser field intensity decreases along radial direction, a short trajectory for one given harmonic will tend to become a cut-off trajectory for that harmonic, thus, it will be generated later in time within the optical cycle. The burst B1 in the far field, as seen from Fig. 3(b). inherits contributions from all B1 bursts emitted along $r$ in the near field. As a result, the resulting chirp and emission time of the far field are determined by these contributions, obviously weighted with the corresponding harmonic flux emission, i.e. intensity times emission area.

*4.2 Robustness of the method*

Bearing in mind a possible practical implementation of the method described here we explored, by numerical modeling, the stability of the SAP generation against the experimental parameters which might depart from the initial conditions, such as chirp and initial CEP, or parameters which might be important for optimizing the harmonic yield, like pulse energy and duration.

At 15 fs pulse duration the SAP is emitted in a wide range of CEP values, extended by roughly 2.5 radians around 0. This means that if one uses pulses of this duration there is no need for CEP stabilization. The pulse duration proves to be critical above 20 fs. At 25 fs a fine CEP tuning is needed to obtain a SAP, which is maintained only in a range of 0.3 rad around the optimum. Even in the optimized case, for this duration we still obtain two small satellites which develop in the half-cycles before and after the main SAP, but the overall energy contained in these satellites is less than 12% of the total energy emitted. Therefore, we conclude that 25 fs is the upper limit for the fundamental pulse duration.

The scheme proves to be extremely stable against the fluctuations of laser intensity. For the 20 fs case, in optimized conditions, the SAP emission is preserved even when the intensity varies by ±30%, which is never the case for now-a-day available Ti:Sa lasers. This stability comes from the method principle: if other parameters are constant the polarization gate is always formed in the same temporal window and the ionization gate is strong so as to deplete the medium in the second part of the pulse. For lower intensities the second spurious peak is stronger, but it still can be eliminated by spatial filtering [28]. For higher intensities the main SAP not only decreases but also becomes longer, due to a larger time interval in which B1 burst is emitted.

The most critical parameter proves to be the chirp induced by passing $E_y$ field through the nonlinear medium. In principle, for a real beam this chirp is not uniform, as the radial variation of the intensity will induce a corresponding variation of the chirp. In an initial stage of our investigation we assumed that the chirp was not radially modulated because one can always expand a beam and use only the central part, minimizing this undesired effect. However this would diminish the method efficiency, thus it is useful to explore the limits of the chirp variation along the radial coordinate. It is shown in Fig. 4. the near field emitted after 1 mm of propagation for different radial modulations of the chirp, keeping other parameters at the values optimized for the constant chirp case. The data show that 5% is the maximum variation of the chirp which the input beam might have across the beam area. This is a clear limitation of the method and in the experimental setup this condition should be fulfilled.

#112585 - $15.00 USD Received 9 Jun 2009; revised 24 Jul 2009; accepted 27 Jul 2009; published 18 Sep 2009

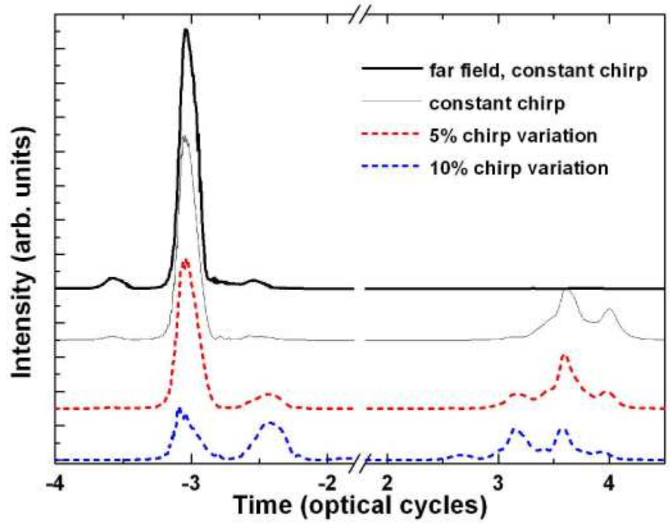


Fig. 4. The near field obtained assuming different degrees of chirp variation along the radial coordinate. The upper pulse shows the far field obtained in constant chirp conditions, by placing a 1.5 mm iris at 0.5 m distance.

Also shown in Fig. 4. is the far field obtained in optimized conditions of uniform chirp, by placing an iris of 1.5 mm diameter at 0.5 m distance. One can see that the second burst formed in the tail of the laser pulse and present in the near field is completely absent in the far field. As mentioned before, the divergence of this second burst is much larger due to the fact that the tail of the laser pulse is strongly defocused by the electron plasma. Thus, the spatial filtering proves to be in this case an additional tool which completes the SAP formation [28].

We also explored the method efficiency compared to that proposed by Sola *et al*. [14], as many experimental conditions are similar, though in our scheme some tricks allow one to generate a SAP from commercially available multi- rather than few-cycle laser pulses, and this implies the additional advantage of potentially using higher peak intensities of the fundamental pulse. In fact, the birefringent method used in [14] to create a polarization gating needs 5 fs pulses and is limited in intensity because the gate is created at pulse center. In modeling we used the optimized conditions specified in [14] for the gating together with the same medium length and pressure. Details of the modeling can be found elsewhere [21]. The result is shown in Fig. 5. where the emitted near fields are plotted as a function of time. The obtained duration is about the same being in the 350-370 as range.

We stress that the Fourier limit of the SAP bandwidth generated with the interferometric scheme, which extends for about 20 harmonic orders from H20 to H40, amounts to $\approx 150$ as when a carrier wavelength of 800 nm is considered. The final duration of $\approx 370$ as results from a double source of pulse lengthening: (*i*) the chirp of harmonics contributing to SAP formation, originated from an intrinsic chirp of the single dipole emission [29–31], which broadens the pulse of $\approx 100$ as, and (*ii*) an additional overall $\approx 120$ as due to the temporal delay between contributions to the SAP coming from points in the near-field having different radial coordinate, as illustrated in Fig. 3. Interestingly, both sources of pulse lengthening can be reduced or even removed. In particular, the intrinsic harmonic chirp can be compensated, while the temporal delay can be diminished by using a top-hat spatial mode for the initial laser beam which minimizes the radial modulation of the laser intensity in the interaction region.

As for the SAP intensity our method yields with a factor of six higher intensity than that used in [14]. This is a remarkable result which is obtained thanks to the principle of the interferometric method, that is, to obtain the SAP at the *best possible time* within the leading edge of the driving pulse. This allows one to tune the intensity to an optimized value which will produce the right ionization fraction. Tuning also the pressure or the interaction length

#112585 - $15.00 USD Received 9 Jun 2009; revised 24 Jul 2009; accepted 27 Jul 2009; published 18 Sep 2009

could enhance even more the SAP intensity. In fact, the signal in Fig. 5. is obtained in conditions similar to that specified in [14] but it is not the maximum signal which can be obtained with the laser parameters and medium length optimized for the interferometric method. We checked that a maximum SAP intensity is obtained after a 2 mm propagation distance and its peak intensity is about 2.5 times larger than the peak of the signal shown in Fig. 5.

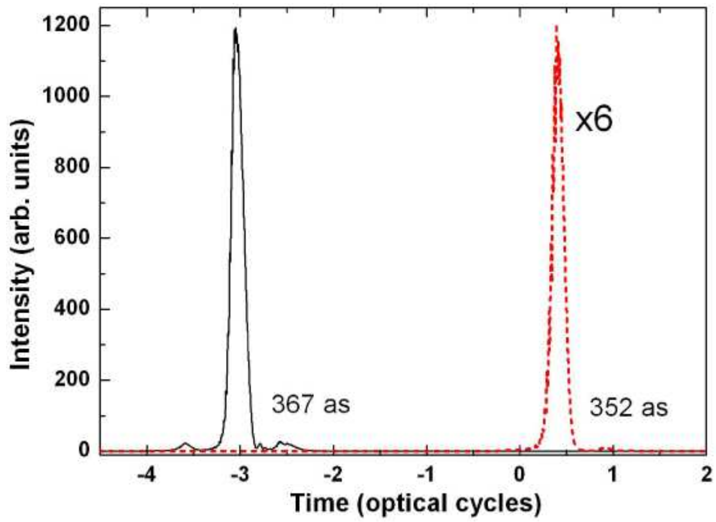


Fig. 5. The time dependence of the near field (black solid line) as compared to the similar signal obtained by modeling the polarization gate method proposed in [14] (red dotted line). Note the amplifying scale factor applied to the later signal. The FWHM durations are also mentioned.

## 7. Conclusions

We performed here a detailed study of the physical mechanisms contributing to SAP generation by using the interferometric scheme reported in [18]. By modeling the laser pulse and harmonic field propagation we obtained a clear picture of the role played by the main physical parameters in the above phenomenon in order to maximize the intensity of the generated SAP. The obtained SAP was also characterized by a short time Fourier transform method to obtain the time-frequency map of the useful signal and to work out the amount of chirp present in the final SAP. For the first time we perform quantum trajectory calculations which can be applied to an arbitrary shape of the laser pulse, and use it to evidence the different phase matching conditions experienced during propagation by different bursts, emitted by the single dipole in different moments,. This kind of analysis is especially useful in polarization gating configurations which create conditions for HHG (SAP) in a very limited window of time.

We finally explored the method to establish its potentials and limits. The most sensitive parameter proves to be the chirp non-uniformity along the radial coordinate, which cannot have variations larger than 5%. We also favorably compared our method with a related one used for few-cycle pulses [14], modeling similar experimental conditions and obtaining a six times larger SAP intensity with about the same duration.


## Acknowledgments

The authors acknowledge financial support from FP7 Project nr. 221952 ATLAS. V. T. and K. K. acknowledge partial financial support from Project PN II IDEI_372.